

# Using MAT\_ADD\_INELASTICITY for Modelling of Polymeric Networks

Fredrik Bengzon<sup>1</sup>, Thomas Borrvall<sup>1</sup>, Anders Jonsson<sup>1</sup>, Magnus Lindvall<sup>2</sup>

<sup>1</sup>DYNAmore Nordic AB

<sup>2</sup>IKEA



Fig. 1 Examples of plastic products and products with polymer components

## 1 Introduction

Thermoplastics are widely used in many industries today. Products such as packaging solutions, consumer goods, medical devices, furniture, electronic devices and vehicles are constantly demanding more and more sophisticated polymer components. In addition, sustainability agendas at many companies today means a necessity to transition from high spec petroleum-based polymers to recycled and biobased alternatives [1]. This creates a pressure on the CAE departments to assess candidate resins at a high pace and make fact-based judgements on their predicted life cycle performance. In a competitive market, there are good reasons to adopt best practice for predicting the life cycle performance of these polymers already during the design phase with the use of realistic simulation.

Advanced rheological network models have changed the game of modelling polymers, offering unmatched predictions simply because the constitutive foundation is based on polymer chain interactions rather than metal elasto-plasticity or linear viscoelasticity (prony). In contrast to elasto-plastic models that were primarily designed to mimic elasticity and dislocation movement in crystalline metal structures, polymers behave fundamentally different and are not fairly characterized with a stress-strain history alone. Typically, polymers are better described as fluids with time, temperature and stress dependency. Any attempt to adopt metal-purpose models for use in polymers, by adding time and temperature data, result in look-up-table type of models that are unfortunately still unable to mimic nontrivial loading scenarios involving time effects. Rheological network models on the other side are fundamentally closer to the micro mechanics of the polymer chain interactions and can therefore naturally handle scenarios such as impact, stress relaxation, creep and recovery in any order and any time span by design. Generally speaking thermoplastics and filled/unfilled elastomers are well suited for this type of modelling approach, especially if one desire to consolidate many existing single purpose models of the same material into a single model (it is not uncommon to use separate models for impact, creep, elevated temperature etc).

The era of non-linear rheological network models began with Bergström-Boyce [2] and Eight-Chain models [3]. Those were commercialized for elastomers with one viscous link which limited the potential use for thermoplastics, but they have been available for two decades in FE-codes. Since then, Jörgen Bergström [4,5] has completely dominated the field of implementation and calibration of rheological network models. The practical usage is based on a licensed third party (subroutine) solution that plugs into major FE-codes. By tailoring the networks for specific families of polymers and elastomers,

remarkable fitting has been shown for multiple complex load cases with emphasis on the time dimension. The concept is based on flexible combinations of springs, advanced dampers, plasticity, Mullins effect, failure and even anisotropy in parallel networks. Among the earliest adopters we find manufacturers of medical and mobile devices, tires and food packages. Hand in hand with the development and availability of sophisticated calibration tools this family of models are gaining more attention and implementation in the industry.

In this paper we present a readily available approach to rheological modeling in LS-DYNA [6], to provide users with simple alternatives to more advanced models [4]. This makes use of a particular branch of the keyword `MAT_ADD_INELASTICITY`, in which fairly general nonlinear viscoelastic network models can be created to capture the time dependent features seen in thermoplastics. In addition, we discuss the aspects of parameter fitting to these kinds of network models as it constitutes an important part of advanced material modeling. Finally we show the viscoelastic effects in a simple application example.

## 2 MAT\_ADD\_INELASTICITY

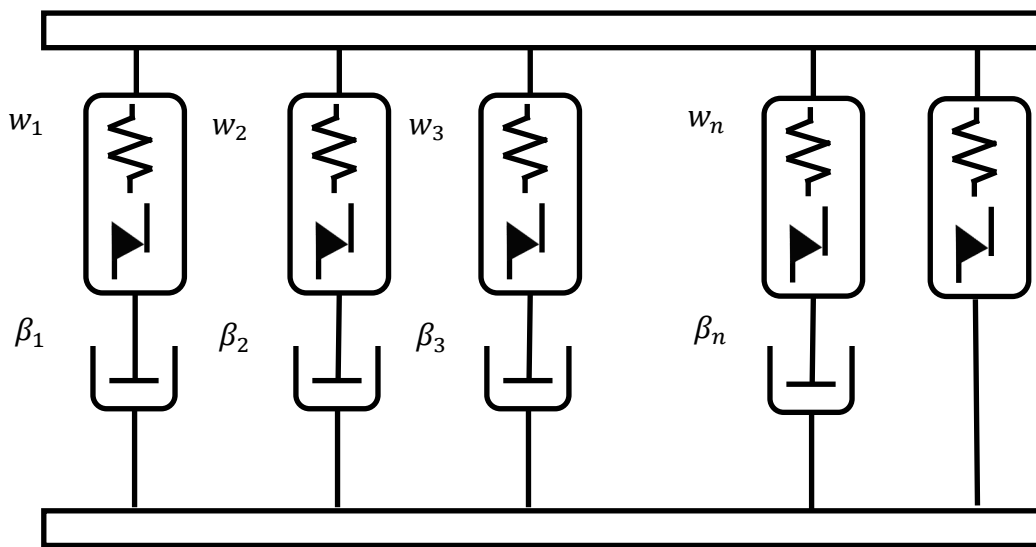


Fig. 2 Rheological description of `MAT_ADD_INELASTICITY`

### 2.1 Background

The keyword `MAT_ADD_INELASTICITY` is intended for complementing standard LS-DYNA material models with inelastic effects in order to enhance their default characteristics. As an example, a promising material model may be complete except for the lack of creep behavior, which is then remedied by adding a viscoelastic model of interest. This usage can be extended to form inelastic *networks* as schematically illustrated in Fig. 2. The general input format and description of the way the inelastic models affect the stress update is explained in detail in the user's manual. The complete exposition is rather comprehensive and here we restrict ourselves to uniaxial deformation and to what is otherwise of interest to us in the context of *polymeric networks*.

### 2.2 Theory and Usage by Example

#### 2.2.1 Base Material

In principle, the way it works is that the user selects a *base material*, which is one of the many standard material models in LS-DYNA. For things to be concrete, we assume SI units and that the base material is a nearly incompressible Neo-Hookean hyperelastic law. The keyword for this is

```
*MAT_HYPERELASTIC_RUBBER
$   mid      ro      pr
$   1        1.e-9   0.4995
$   c10
```

5.e6

which means that the infinitesimal shear modulus is  $G = 10 \text{ MPa}$ . Upon execution and for a given (uniaxial) deformation, this material provides a (uniaxial) stress  $\sigma_0$  in accordance with the energy potential, and the (time) evolution of this stress is used as input for the viscoelastic links to be explained next.

### 2.2.2 Inelastic Addition

An example of a simple inelastic plug-in to the material above is

```
*MAT_ADD_INELASTICITY
$      mid  nielinks          g
      1      1          1.e7
$  nielaws  weight
      1      0.8
$      law  model
      6      4
$              s          p          q          e
              1.e6          6          -.3      0.0001
```

where the parameter `mid` references the base material by means of having the same material identity, and the other parameters will be explained hereafter.

### 2.2.3 Links

The user should specify a certain number of inelastic *links* (`nielinks`) and an estimate of the infinitesimal shear modulus (`g`) of the base material<sup>1</sup>. Here we only specify one link, and the stress evolution for that link is (because of choices made in section 2.2.5) given as

$$\dot{\sigma}_1 = \dot{\sigma}_0 - \beta_1 \sigma_1. \quad (1)$$

Here  $\beta_1$  is the *relaxation coefficient* which in turn has the expression

$$\beta_1 = \frac{E}{\sigma_1} \dot{\varepsilon}_1 \quad (2)$$

and  $\varepsilon_1$  is the *creep strain* for the link in question, which requires a constitutive law to be specified in Section 2.2.5.

### 2.2.4 Weights

Each link must be associated with a relative *weight* (`weight`) between zero and one, and the weights for all inelastic links should sum up to something less than one. Whatever remains after summation is the relative weight given to the purely elastic link. In this example, the only link provided is given a weight of  $w_1 = 0.8$ , or 80%. This in turn means that the remaining elastic link is given a relative weight of  $w_0 = 1 - w_1 = 0.2$ , or 20%, and the resulting stress of this particular material is

$$\sigma = w_0 \sigma_0 + w_1 \sigma_1 = 0.2 \sigma_0 + 0.8 \sigma_1. \quad (3)$$

Furthermore, the number of *laws* used in each link (`nielaws`) must be specified. While this in general could be many, we are here interested in using a single law for each link and this parameter is set accordingly.

### 2.2.5 Laws

The *law* (`law`) for each link is in this paper specified as a *viscoelastic* law, meaning it will always have a value of 6. The specific *model* (`model`) within this family is specified to either 4 (Norton-Bailey) or 5 (Bergström-Boyce), which determines the evolution of creep strain. For Norton-Bailey we have

---

<sup>1</sup> The shear modulus  $G$  is required for the general stress update, which is specified in terms of the deviatoric stress. For uniaxial deformation, and for making things more understandable, think of it as specifying the Young's modulus  $E$ .

$$\dot{\varepsilon}_1 = \left( \left( \frac{\sigma_1}{\sigma_*} \right)^{p_*} \left( (q_* + 1)(\varepsilon_* + \varepsilon_1) \right)^{q_*} \right)^{\frac{1}{q_*+1}} \quad (4)$$

and for Bergström-Boyce

$$\dot{\varepsilon}_1 = (\lambda_c - 1 + \varepsilon_*)^{q_*} \left( \frac{\sigma_1}{\sigma_*} \right)^{p_*} \quad (5)$$

and  $\lambda_c \geq 1$  is the creep stretch<sup>2</sup>. The index for the parameters  $\{\sigma_*, p_*, \varepsilon_*, q_*\}$  in equations (4-5) are dropped for simplifying the expression, but if more than one link is used then obviously each link will have a unique set of values for these parameters. In this hypothetical case the values are

$$\sigma_* = 1 \text{ MPa}, p_* = 6, \varepsilon_* = 10^{-4}, q_* = -0.3. \quad (6)$$

### 2.3 Small Deformations

While the previous section is a simplified, and somewhat incomplete, description of the model, it is rather straightforward to depict the general situation. Merely replace the subindex „1“ in equations (1-5) by  $i$  and let it range across all  $n$  links. For small deformations, assuming the base material has a stress update of the form

$$\dot{\sigma}_0 = E \dot{\varepsilon}, \quad (7)$$

we can combine equations (1-3) and (7) to see that

$$\dot{\sigma} = \sum_{i=0}^n w_i \dot{\sigma}_i = \sum_{i=0}^n w_i (\dot{\sigma}_0 - \beta_i \sigma_i) = \sum_{i=0}^n w_i \left( E \dot{\varepsilon} - \frac{E}{\sigma_i} \dot{\varepsilon}_i \sigma_i \right) = E \left( \dot{\varepsilon} - \sum_{i=0}^n w_i \dot{\varepsilon}_i \right) = E (\dot{\varepsilon} - \dot{\varepsilon}_l) \quad (8)$$

where  $\varepsilon_l$  can be seen as the *weighted* creep strain across all links. Here we have set  $\dot{\varepsilon}_0 = \beta_0 = 0$  for the purely elastic link, and in the end we note that the combination of nonlinear viscoelastic laws results in a stress update familiar from the theory of inelasticity in general.

## 3 Parameter Fit

### 3.1 Preliminaries

A good set of material parameters is essential for taking advantage of the richness this material model offers. Needless to say, the fit in itself is nontrivial and to begin with we are obliged to answer at least the questions in the following subsections. The answers will probably vary depending on the source providing them, and here we combine general guidelines from the literature with our own experience.

#### 3.1.1 What base material should be used?

As far as the base material is concerned, it makes sense to use a hyperelastic material of relatively low order. The basis for this assumption is our belief that the nonlinear effects this polymeric material exhibits stem primarily from viscous and/or plastic phenomena rather than nonlinear elasticity. To this end we have selected a nearly incompressible Neo-Hookean model where the Poisson's ratio is set to 0.495 and the shear modulus is subject for fitting. The incompressibility can be debated, and while there may be reasons to allow compressible behavior we admit that our choice is in part motivated by simplicity.

#### 3.1.2 How many links should we use?

In addition to the purely elastic component, we use between three and five viscous links to incorporate the nonlinear effects. It has been suggested that this provides the potential to represent the physical material well enough without adding redundancy to the model, and we find no reason to doubt this claim.

#### 3.1.3 What (non)linear model(s) should the links be composed of?

To the best of our knowledge, Norton-Bailey and Bergström-Boyce are the models of choice in this context. As an interesting comparison we intend to fit both models to the test data in order to deduce

<sup>2</sup> The notation in equations (4-5) differs from that in the manual [6], consistency is maintained throughout the paper though, and hopefully it won't add too much confusion to the general understanding of the models.

which one of the two work horses provides the best fit in this case. It should be emphasized that we do not draw general conclusions from this rather non-scientific experiment.

### 3.1.4 What tests should the fit be based upon?

The tests for fitting a material model should in principle be conducted so that the test results, in some sense, span the deformation realm the material is subjected to when used for its intended application. This not only includes particular directions of deformation but also rate and relaxation effects. For simplicity we consider uniaxial tests and focus is turned to capturing the viscous behaviour of the material. We have decided to use three types of tests; a uniaxial test, uniaxial tests with relaxation/creep and a cyclic test. To be specific, we performed three different tests with relaxation/creep, so the total number of tests conducted are five and they will be presented in detail at the end of this section.

### 3.1.5 What parameters can be selected a priori and which ones should be subject for optimization?

The links in Norton-Bailey and Bergström-Boyce have a similar set of parameters, these are

- Relative weights  $w_1, w_2, \dots, w_n$ , restricted by the conditions  $0 < \underline{w}_i \leq w_i \leq \overline{w}_i \leq 1$  and  $\sum_{i=1}^n w_i = \overline{W} < 1$ . These weights determine the influence a certain link has on the overall behaviour.
- Stress exponents  $p_*$  and normalization stress levels  $\sigma_*$ . Naturally, these are subjected to similar constraints,  $1 < \underline{p}_* \leq p_* \leq \overline{p}_* < \infty$  and  $0 < \underline{\sigma}_* \leq \sigma_* \leq \overline{\sigma}_* < \infty$ , and are used for characterizing the relaxation effects influenced by the stress level.
- Strain exponents  $q_*$  with constraints  $-1 < \underline{q}_* \leq q_* \leq 0$ , used for strain dependent relaxation behavior.

These parameters are variables in the optimization algorithm while all others,  $\varepsilon_*$  and  $G$ , are set in advance. Before turning the attention to the algorithm used for the fit, here is a description of the test cases.

## 3.2 Test Cases

The material used for the fitting experiment is a Low Density PolyEthylene (LDPE), commonly used for products in the consumer and medical industry, and the test data was provided by Tetra Pak. See [7] for more info. Stress is in *MPa* and Time is in *seconds* if nothing else is stated.

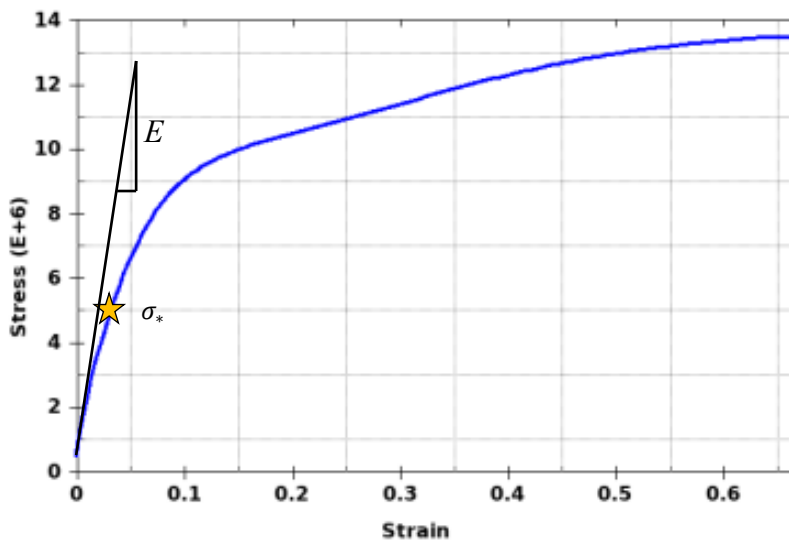


Fig. 3 Uniaxial Test, initial stiffness  $E$  and guess of  $\sigma_*$  are indicated

### 3.2.1 Uniaxial Tension

The first test is uniaxial tension, see Fig. 3, where the specimen is loaded at a rate of  $3\% s^{-1}$  until it fails at a strain of about 66%. This is the one test that perhaps should be left out of the mix since it

most certainly incorporates effects that are not represented by the material model at hand. Nevertheless, it is included by a completeness argument.

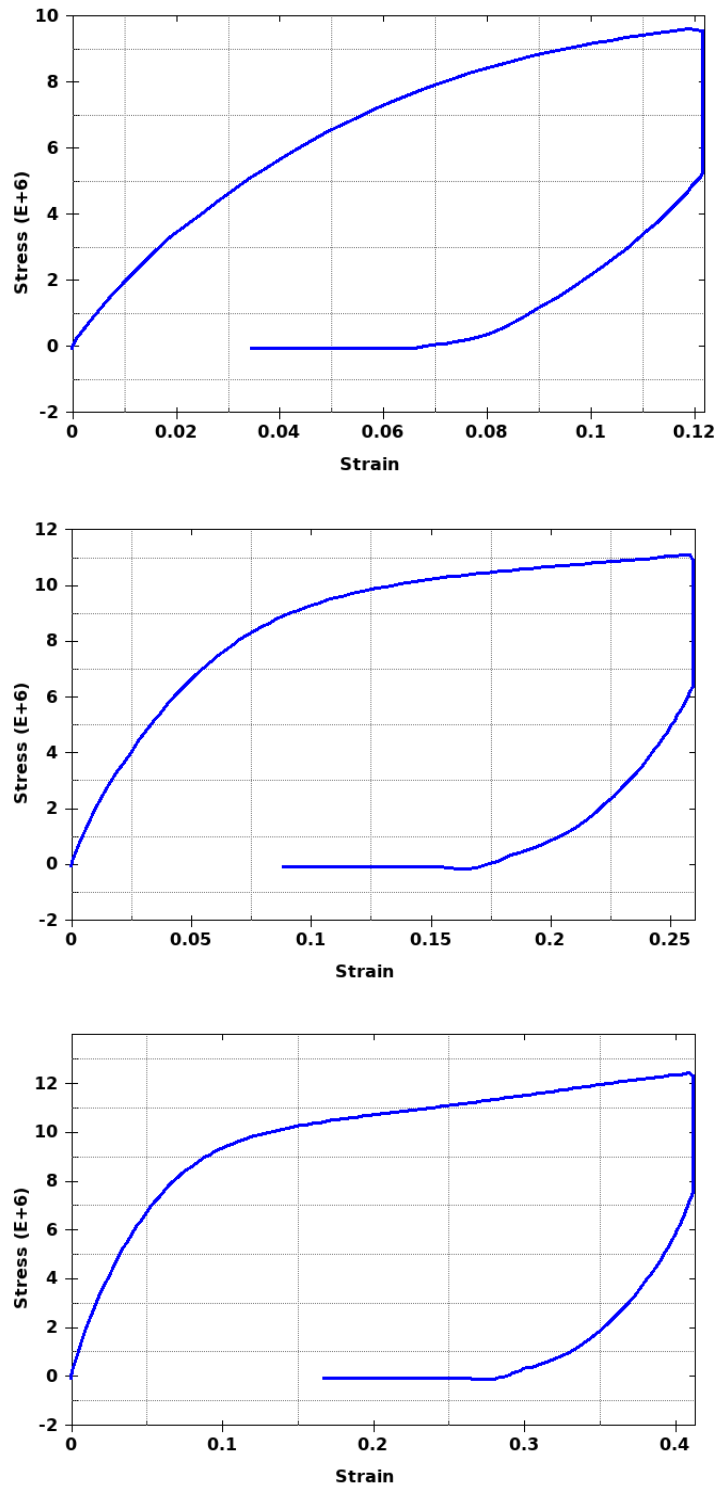


Fig. 4 Relaxation/Creep Tests

### 3.2.2 Uniaxial Tension with Loading-Relaxation-Unloading-Creep

Three uniaxial tension tests with relaxation and creep are included, see Fig. 4, where the specimen is loaded at a rate of  $3\% s^{-1}$  up to a strain of 12.2%, 26% and 41.3%, respectively. After that, the

specimen is held at constant strain while the stress is allowed to relax for one hour. After that, the specimen is unloaded to its stress free configuration at a rate of approximately  $3 \text{ MPa/s}$  after which it recovers at zero stress for about 20 minutes.

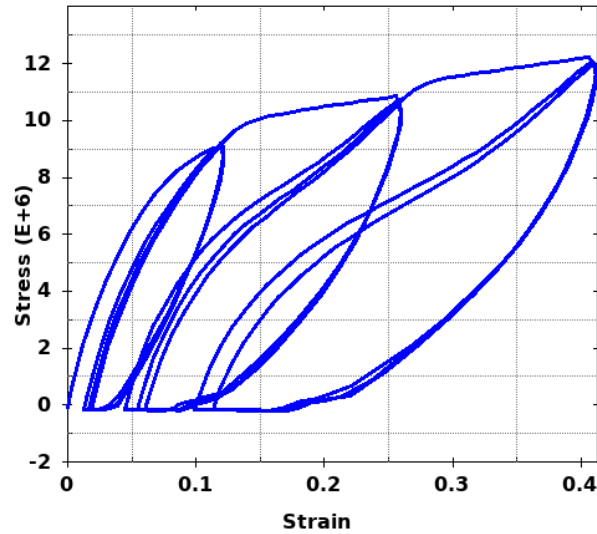


Fig. 5 Cyclic Test

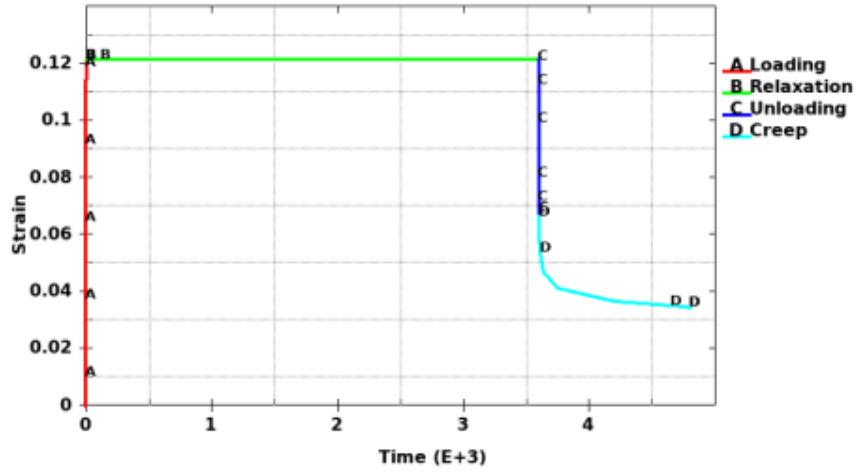
### 3.2.3 Cyclic Loading and Unloading

The final test is a test where the specimen undergoes nine cycles of loading and unloading, see Fig. 5. The loading rate is  $3\% \text{ s}^{-1}$  and the unloading rate is about  $3 \text{ MPa/s}$ . The first three cycles peak at a strain of 12.2%, the next three at 26% and the final three at 41.3%. Between each cycle, the specimen is at rest for 1 minute.

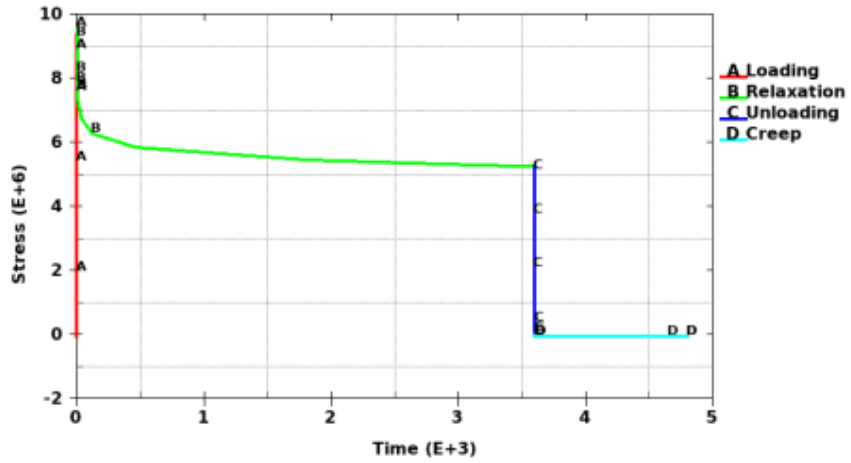
### 3.3 Algorithm

From an engineering point of view, a set of material parameters is deemed decent if test and simulation data match well enough on mere ocular inspection. That is, the model should capture the characteristic features of the material and corresponding response curves should be close. Given the complexity of this particular material model and the amount of test data required, a trial-and-error approach for finding such a set appears hopeless. We are therefore at the mercy of optimization algorithms to accomplish this task. In this paper we use an in-house code for parameter fitting for which the algorithm is described in detail, and compare this with results obtained with the commercial software MCalibration. For the latter we refer to [5] and related documentation.

a)



b)



c)

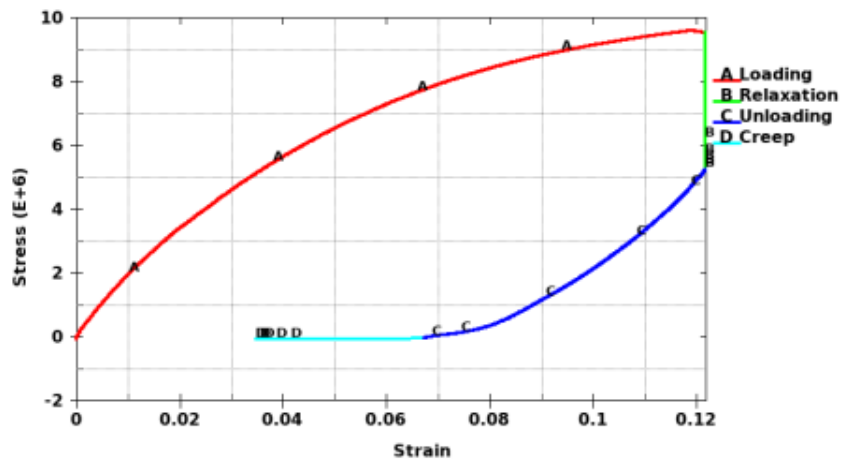


Fig. 6 Sequences from first relaxation/creep test



### 3.3.1 Objective

An optimization problem requires an *objective* function with the property that a perfect match between test and simulation data results in a merit value of zero. It should also return increasingly larger values as the correlation between test and simulation gets worse. Once this function is determined, the task is to minimize it with respect to the constraints discussed in the next section. It is by no means straightforward to determine it in a way that “small” function values correlate well with plausible results from an engineering point of view, but here is one approach to that challenge.

The intuitive choice is that of a nonlinear least squares function, where the response from all tests are combined to form an error measure to be minimized. Because of the large time scale differences in the tests, i.e., loading/unloading in seconds and relaxation/creep in hours, it must be carefully designed to properly account for each phase in each test. To this end, we split the response curves in *sequences*, as exemplified in Fig. 6. The first sequence is the loading phase, represented by curve A, and the second sequence is the holding phase during which stress relaxation occurs, represented by curve B. Then unloading follows in the third sequence, curve C, and the test ends with a phase where the strain creeps at zero stress, curve D. For each sequence we compute an error of the form

$$c = \sqrt{\frac{1}{T} \int_0^T (f - g)^2 dt}. \quad (9)$$

Here we use  $T$  to denote the time duration for the sequence,  $f = f(t)$  is the result from simulation and  $g = g(t)$  is the result from test, both functions of time  $t$ . This provides a time independent merit, so a sequence performed in seconds is given similar attention to that performed in hours. Applying (9) to all tests and all sequences gives a bunch of  $c_j^j$ , where  $J$  ranges over all tests while  $j$  ranges over all sequences within those tests. The objective function is then composed as

$$o = \sum_J \gamma_J \{ \sum_j \delta_j^j c_j^j \} \quad (10)$$

with  $\gamma_J$  and  $\delta_j^j$  being selected weights for strengthening or weakening the influence of some tests and/or sequences.

The weights in (10) may for the sake of simplicity be chosen as unity, which means that each sequence is equally important. A problem arises when a prescribed motion in the first sequence is followed by a prescribed force in the second, which happens for instance in the loading/unloading situation in Fig. 6. For the first/second sequence, the curves to be compared are that of reaction forces due to the prescribed motion, i.e., corresponding to curve A/B in b). For the third/fourth sequence the curves to be compared are the creep displacements due to the change in force, i.e., curve C/D in a). This means that units are mixed in (10), and as a consequence the  $\delta_j^j$  must be adjusted for that. This adjustment was based on trial-and-error to fine-tune the relative importance between the different sequences, and in the end the stiffness factor used for this purpose was  $10^4 Pa$  in all such terms.

### 3.3.2 Constraint

For our material model to make physical sense, we need bounds on the design variables (material parameters) and make sure that the sum of weights does not exceed unity. This was formally discussed in Section 3.1.5, and the values we use are

$$\overline{W} = 0.95 \quad (11a)$$

$$\underline{w}_j = 0.01 \quad (11b)$$

$$\overline{w}_i = 1 \quad (11c)$$

$$\underline{\sigma}_* = 1 MPa \quad (11d)$$

$$\overline{\sigma}_* = 100 MPa \quad (11e)$$

$$\underline{p}_* = 1.1 \quad (11f)$$

$$\overline{p}_* = 12 \quad (11g)$$

$$\underline{q}_* = -0.99 \quad (11h)$$

### 3.3.3 Constants

The strain perturbation is arbitrarily set to  $\varepsilon_* = 10^{-4}$  in our optimization, while the choice of  $G$  will be discussed in the next section.

### 3.4 Results and Discussion

#### 3.4.1 Strategy

A multitude of fitting experiments were conducted in order to gain experience and develop a reasonable strategy for optimal fitting. In general it is safe to say that the parameters obtained depend to a large extent on the selection of weights in (10) as well as the initial guess. Different optimization tools are likely to find different parameters simply because of ambiguities in how the optimization problem is setup. In particular the inclusion or exclusion of the cyclic test has a large influence on the final result, this particular observation will be discussed further below. The strategy we developed was partly based on engineering intuition but also drew from what we learned during early attempts. We find it general enough to be applicable for other materials and can be described as follows.

1. Select between 3 and 5 inelastic links, in our case we use 4. The intention is to reserve at least one of the links to represent plasticity and the other to represent viscous effects.
2. Set  $G$  to  $E/3$ , where  $E$  is the initial slope in the stress vs. strain curve for the uniaxial test. This parameter is indicated in Fig. 3 and is in our case fixed to  $80 \text{ MPa}$ .
3. Set each of the normalization stresses  $\sigma_*$  to 50% of initial yield in the uniaxial tension test, this point is highlighted in Fig. 3 and set to  $5 \text{ MPa}$  for this material.
4. Distribute the weights  $w_i$  evenly and so that they sum to roughly 90-95%, we used the value 0.23 for each link.
5. Let the stress exponents  $p_*$  increase from 1 and 12 to represent a fair distribution of viscoelasticity and plasticity. We used the values 1.5, 3, 6 and 12.
6. Set the strain exponents  $q_*$  to zero.

This should provide a decent initial guess for the optimization problem. At this point, we decide to fit the material parameters to the uniaxial and relaxation tests, thus omitting the cyclic test. Before justifying this approach, we present the results from this partial solution.

#### 3.4.2 W/O Cyclic Test

As a further refinement and independently of the in-house approach to the problem, the runs with MCalibration were performed in steps during which some parameters were held fixed. To be specific, the steps were

1. Optimize wrt weights  $w_i$  and stress factors  $\sigma_*$  only.
2. Optimize wrt stress exponents  $p_*$  only.
3. Optimize wrt stress exponents  $p_*$ , weights  $w_i$  and stress factors  $\sigma_*$  only.

Note that MCalibration for practical reasons was run entirely with displacement driven loadcases even though the actual experiments were driven with a mix of displacement and force sequences. This influences the appearance of the resulting fitting between MCalibration and in-house calibration since deviations show up as stress deviations in one case and strain deviation in the other. Also note that the strain exponents  $q_*$  are held fixed with this approach. The line of thought is to gradually approach the optimum with the purpose of avoiding any local minima, whether this refinement is necessary has not been experimentally verified. The results are shown in Fig. 7, in which the notation and units differ from what has been presented here, so here is a recapitulation of the parameter values.

$$w_1 = 0.200 \quad (12a)$$

$$\sigma_1 = 5.48 \text{ MPa} \quad (12b)$$

$$p_1 = 1.32 \quad (12c)$$

$$w_2 = 0.311 \quad (12d)$$

$$\sigma_2 = 4.58 \text{ MPa} \quad (12e)$$

$$p_2 = 3.07 \quad (12f)$$

$$w_3 = 0.217 \quad (12g)$$

$$\sigma_3 = 4.08 \text{ MPa} \quad (12h)$$

$$p_3 = 5.41 \quad (12i)$$

$$w_4 = 0.190 \quad (12j)$$

$$\sigma_4 = 6.39 \text{ MPa} \quad (12k)$$

$$p_4 = 20.0 \quad (12l)$$

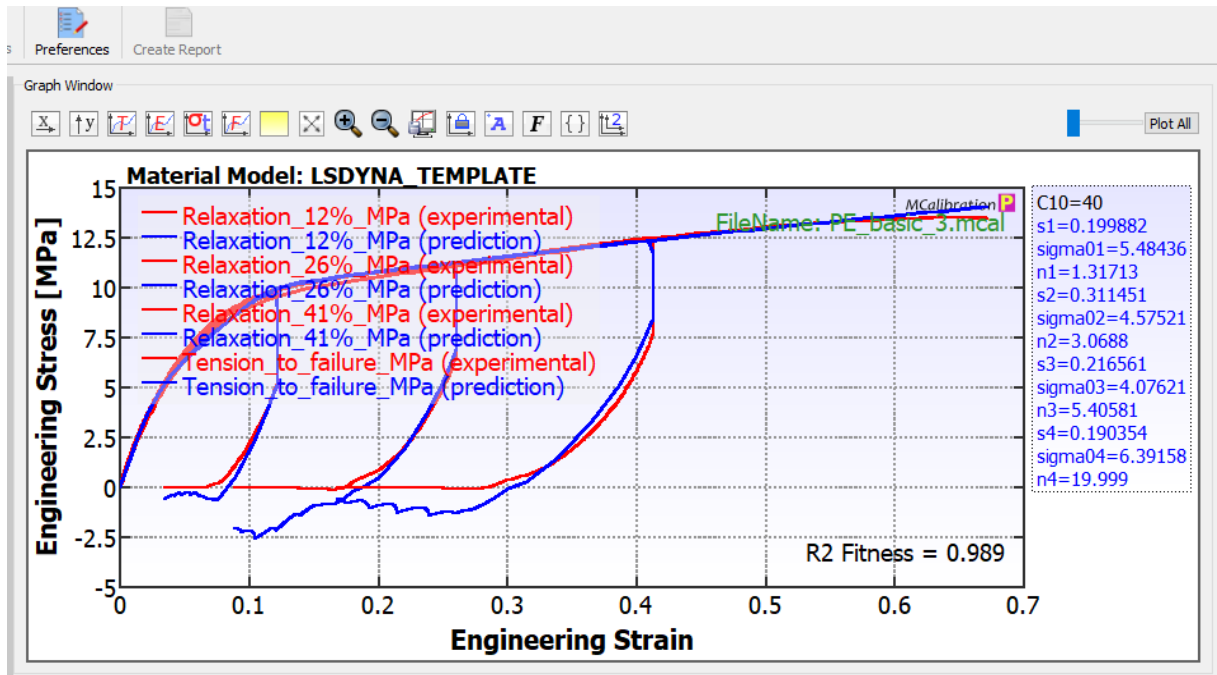


Fig. 7 Results from MCalibration

The fit is excellent, except for discrepancies during sequence three and four (unloading and creep) in the relaxation tests.

The alternate fitting schemes from the in-house approach resulted in the following parameters for Norton-Bailey

- $w_1 = 0.356$  (13a)
- $\sigma_1 = 39.9 \text{ MPa}$  (13b)
- $p_1 = 1.10$  (13c)
- $q_1 = 0$  (13d)
- $w_2 = 0.257$  (13e)
- $\sigma_2 = 20.3 \text{ MPa}$  (13f)
- $p_2 = 1.10$  (13g)
- $q_2 = 0$  (13h)
- $w_3 = 0.227$  (13i)
- $\sigma_3 = 7.30 \text{ MPa}$  (13j)
- $p_3 = 6.14$  (13k)
- $q_3 = 0$  (13l)
- $w_4 = 0.0895$  (13m)
- $\sigma_4 = 5.65 \text{ MPa}$  (13n)
- $p_4 = 12.0$  (13o)
- $q_4 = -0.956$  (13p)

and for Bergström-Boyce in

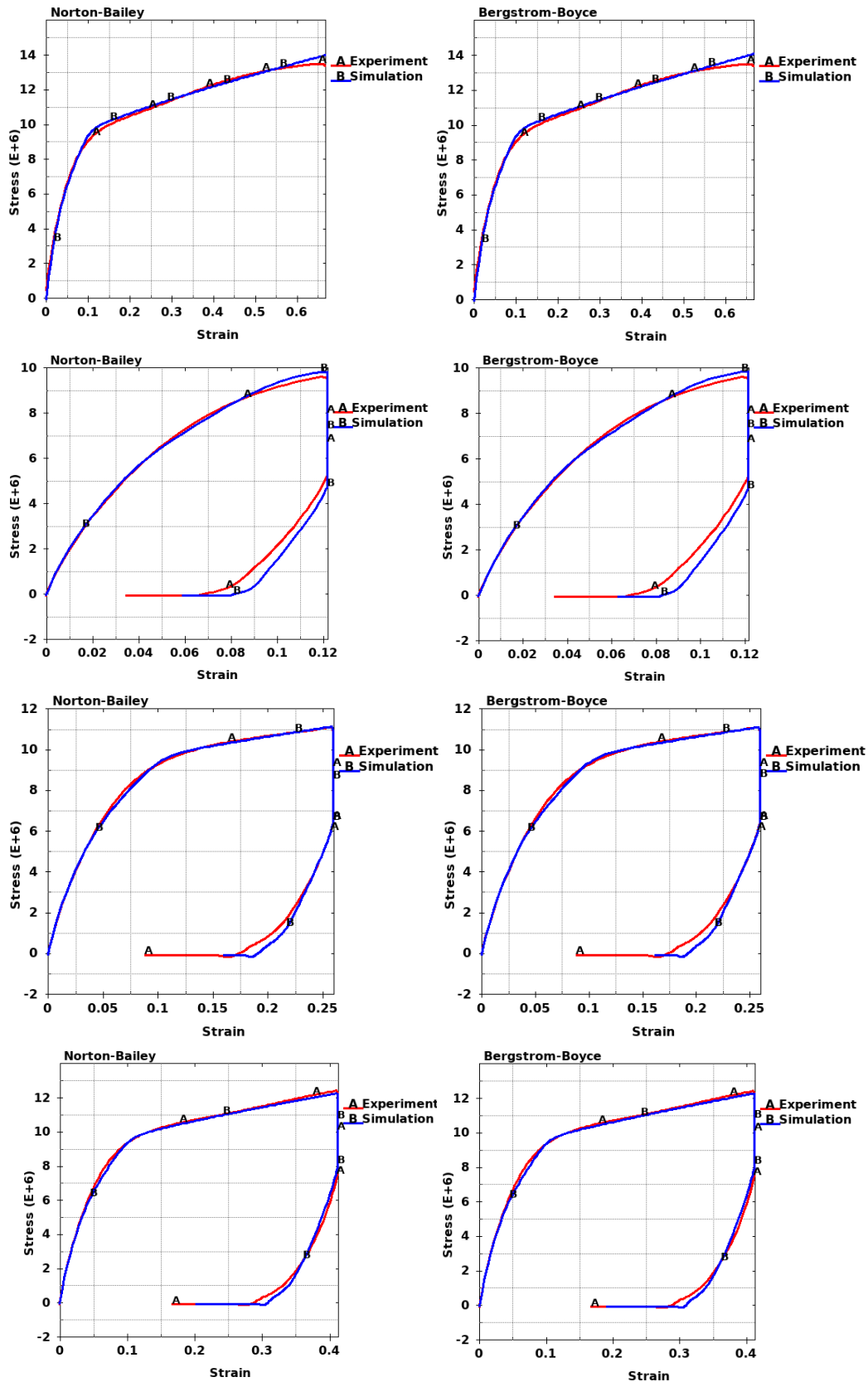


Fig. 8 Fitted data for Norton-Bailey (left) and Bergström-Boyce (right)

$w_1 = 0.307$	(14a)
$\sigma_1 = 20.4 \text{ MPa}$	(14b)
$p_1 = 1.18$	(14c)
$q_1 = 0$	(14d)
$w_2 = 0.275$	(14e)
$\sigma_2 = 19.2 \text{ MPa}$	(14f)
$p_2 = 1.22$	(14g)
$q_2 = 0$	(14h)
$w_3 = 0.230$	(14i)
$\sigma_3 = 5.03 \text{ MPa}$	(14j)
$p_3 = 12.0$	(14k)
$q_3 = 0$	(14l)
$w_4 = 0.108$	(14m)
$\sigma_4 = 4.99 \text{ MPa}$	(14n)
$p_4 = 12.0$	(14o)
$q_4 = 0$	(14p)

and the resulting curves are shown in Fig. 8. As can be seen from these curves, the two models seem to provide a reasonable fit given these presuppositions. The objective values are 251224 for Norton-Bailey and 338004 for Bergström-Boyce, respectively, which from a mathematical standpoint means that the former provides a better fit. Examining the resulting material parameters, we note the following

- The first two links in Norton-Bailey as well as Bergström-Boyce tend towards linear viscoelastic links, as the exponents  $p_1$  and  $p_2$  either attain the lower bound or are close to it. These two links might be replaced by a single link, since both appear to model the response on a relatively short time scale.
- The third link in Norton-Bailey appears to be an important contribution to the fit, because of the stress activation level and moderate size of stress exponent.
- The final two links in Bergström-Boyce appear to model the same plastic response and can probably be replaced by a single link.
- The only indication of a strain dependent response is in the fourth link of Norton-Bailey, which given the high stress exponent is a plastic link. Given the extreme exponent, it may be something for fine-tuning the fit.

The conclusion is that for four links, many different parameter settings are adequate for representing the loading and relaxation response of this material. What is not obvious from the graphs is how well the unloading and creep phases are fitted. One thing to observe is that the residual strain in all relaxation tests is overestimated by the fitted materials. In retrospect our assumption is that the MCalibration optimization had a somewhat unbalanced data point distribution, for which the latter parts of the experiments (unloading and creep) are given less attention in the fit. For the alternate method it comes down to the choice of weight factors, and presumably the load driven phases are not given sufficient importance. However, decreasing this weight factor, see discussion at the end of Section 3.3.1, will probably worsen the results from the displacement driven phases.

### 3.4.3 *W* Cyclic Test

Adding the cyclic test, and starting the optimization from the parameters obtained in the previous section, gives the following for Norton-Bailey

$w_1 = 0.409$	(15a)
$\sigma_1 = 40.7 \text{ MPa}$	(15b)
$p_1 = 1.10$	(15c)
$q_1 = 0$	(15d)
$w_2 = 0.283$	(15e)
$\sigma_2 = 38.5 \text{ MPa}$	(15f)
$p_2 = 1.10$	(15g)
$q_2 = 0$	(15h)
$w_3 = 0.109$	(15i)
$\sigma_3 = 3.73 \text{ MPa}$	(15j)

$$\begin{aligned}
 p_3 &= 6.57 & (15k) \\
 q_3 &= 0 & (15l) \\
 w_4 &= 0.131 & (15m) \\
 \sigma_4 &= 6.51 \text{ MPa} & (15n) \\
 p_4 &= 12.0 & (15o) \\
 q_4 &= -0.775 & (15p)
 \end{aligned}$$

and for Bergström-Boyce

$$\begin{aligned}
 w_1 &= 0.333 & (16a) \\
 \sigma_1 &= 12.2 \text{ MPa} & (16b) \\
 p_1 &= 1.43 & (16c) \\
 q_1 &= 0 & (16d) \\
 w_2 &= 0.275 & (16e) \\
 \sigma_2 &= 11.9 \text{ MPa} & (16f) \\
 p_2 &= 1.60 & (16g) \\
 q_2 &= 0 & (16h) \\
 w_3 &= 0.140 & (16i) \\
 \sigma_3 &= 2.20 \text{ MPa} & (16j) \\
 p_3 &= 12.0 & (16k) \\
 q_3 &= 0 & (16l) \\
 w_4 &= 0.172 & (16m) \\
 \sigma_4 &= 7.54 \text{ MPa} & (16n) \\
 p_4 &= 12.0 & (16o) \\
 q_4 &= 0 & (16p)
 \end{aligned}$$

The first four tests are not affected so much, only small adjustments to that of Fig. 8. The resulting fit for the cyclic test is shown in Fig. 9, which we intend to discuss.

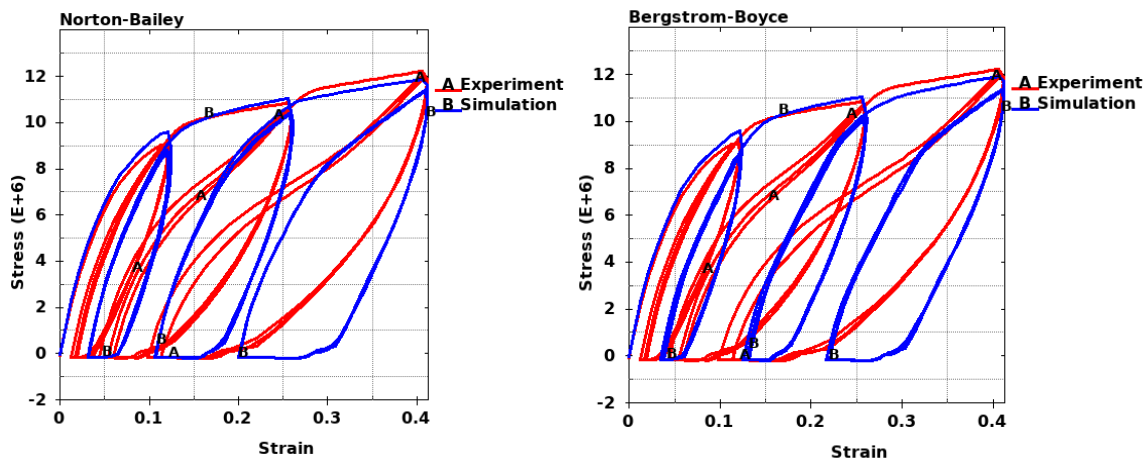


Fig. 9 Results from cyclic test

Apparently, the model is not capable of accurately fitting the cyclic test, indicating either (i) lack of physics in the model, (ii) entrapment in local optimum or (iii) insufficient number of links. We have run enough optimizations to discard the hypothesis of this being caused by a local optimum, and since the resulting parameters in equations (15-16) indicate a linear dependence between at least the first two links we also believe that adding more will not improve this situation. We therefore lean towards the first of these explanations, thinking that the amendment of a Mullins effect might improve the situation. This is speculative, but might be something to consider in a continuation of this work.

#### 3.4.4 Observations

Comparing results from MCalibration and the documented algorithm should be taken lightly, as it turns out that the prerequisites for the fitting were different. The base model was different in that of a different model and Poisson's ratio (Mooney-Rivlin model with  $\nu = 0.49$  vs Hyperelastic Rubber with  $\nu = 0.4995$ ), and presumably the merit function is different between the two approaches. Also, the

strain exponents were not optimized with MCalibration, the intention is rather to show that both are valid approaches to fitting rheological network models.

The optimization in the previous section was also performed *without* the pre-optimization presented in Section 3.4.2, i.e., the cyclic test was included from the get-go starting with the initial guess given at the beginning of Section 3.4.1. It turns out that the result is the same in terms of an almost identical objective value, and a conclusion is likely that the pre-optimization is unnecessary. It is however confirmed that the initial guess has an influence of the result and it may be worthwhile to develop an alternate strategy where several optimizations are performed starting from different initial guesses. Nevertheless, the most important aspect is to provide the optimization tool with a model that captures the real physics of the material, which is not the case when including the cyclic test. Once such a model is cemented, it may turn the tables in terms of how a strategy should be designed.

#### 4 Example

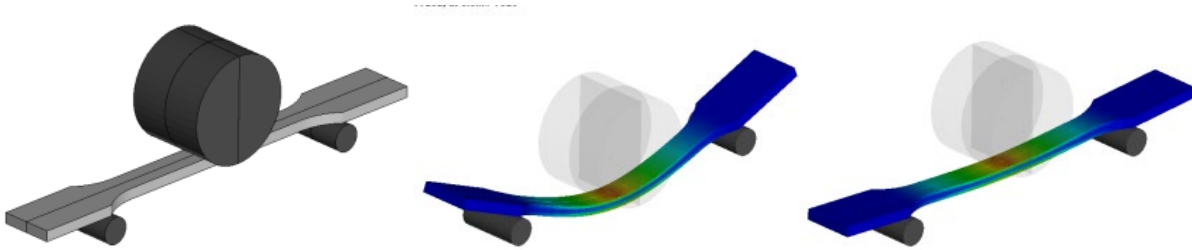


Fig. 10 Dogbone subjected to gravity load

Consider a representative scenario of the life cycle of a plastic component. It could be subjected to

- sudden loading (snapping, mounting, impact)
- creep
- stress relaxation
- unloading
- recovery

Typically, we may want to run these loads in

- an arbitrary sequence
- using implicit solver
- with contacts
- with a reasonable simulation time

The demonstration case includes all mentioned aspects and was constructed and computed with two alternative material models based on the PolyEthylene test data presented in Section 3.2. one using the inelastic model fitted in Fig. 7 and one using the piecewise plasticity material model 24. More specifically, the dogbone in Fig. 10 is subjected to a 300g weight that is instantly applied and kept for one hour during which the creep deformation is observed. A rigid body stopper limits the displacement of the body to 15 mm. After that the weight is removed, and the dogbone recovers for yet another hour.

The response is given in Fig. 11, in terms of displacements of the weight and contact force between the weight and dogbone. First, the plastic material shows a stationary equilibrium point and a permanent deformation due to some plastic strain, which is not correlating with thermoplastic behavior over this range of time. The rheological material, however, creeps quickly during the first few seconds to reach the maximum displacement. While the dogbone is kept at this location, the stress relaxes as can be seen from the decay of contact force. The sudden removal of the weight after one hour causes the material to recover during the second half of the simulation, resulting in a permanent deformation that is attributed to the links with high stress exponents. This example qualitatively shows the viscous effects pertaining to thermoplastics and stresses the importance of including this element of reality in the modelling of these materials.

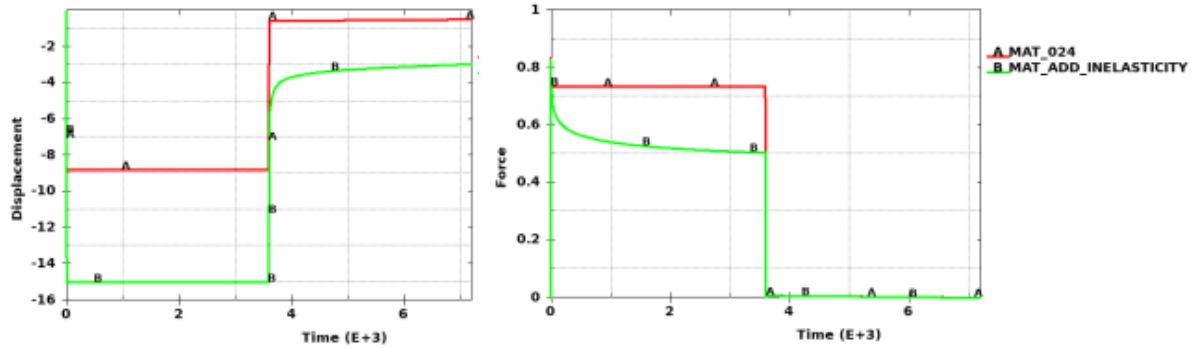


Fig. 11 Rigid body displacement and contact force for plastic and rheological material

## 5 Summary

An approach to rheological modelling of polymeric networks that employs a particular branch of MAT\_ADD\_INELASTICITY has been presented. It is shown that models within this framework are capable of representing the basic viscoelastic features observed in thermoplastics, e.g., creep and relaxation, including nonlinear strain and stress effects. The intention is to make a valid assessment of the life-cycle performance of a plastic product in its area of use. A thorough elaboration on parameter fitting was provided in hope that it paves the way towards a complete treatment, from calibration to simulation, of these models. The work shows that the nonlinear viscoelastic models available in LS-DYNA (Norton-Bailey and Bergström-Boyce) allow for a good fit to loading and relaxation data, whereas more complex loading and unloading scenarios presumably requires additional physics to be implemented.

## 6 Acknowledgements

The authors are grateful to Eskil Andreasson and Viktor Petersson at Tetra Pak for providing the experimental test data used in this publication.

## 7 Literature

- [1] Petersson V., Andreasson E. and Persson-Jutemar E. *Towards Sustainable Plant Based Packages*, Proc. NAFEMS conference Simulation Driven Design , 2019.
- [2] Bergström J. and Boyce M. *Constitutive modeling of the large strain time-dependent behavior of elastomers*, J. Mech. Phys. Solids **46**, pp. 931-954 (1998).
- [3] Arruda E. and Boyce M. *A three-dimensional constitutive model for the large stretch behavior of rubber elastic materials*, J. Mech. Phys. Solids **41**, pp. 389-412 (1993).
- [4] PolymerFEM, <https://polymerfem.com>
- [5] MCalibration, <https://polymerfem.com/mcalibration>
- [6] LS-DYNA Keyword User's Manual
- [7] Kroon, M., Andreasson E., Persson-Jutemar E. and Petersson V. *Anisotropic Elastic-Viscoplastic Properties at Finite Strains of Injection-Moulded Low-Density Polyethylene*, Exp Mech **58**, pp. 75–86 (2018).